Cytotoxic activity of *Crotalus molossus molossus* snake venom-loaded in chitosan nanoparticles against T-47D breast carcinoma cells

Jorge Jimenez-Canale[1#], Daniel Fernández-Quiroz[2#], Nayelli G. Teran-Saavedra[1], Kevin R. Diaz-Galvez[1], Amed Gallegos-Tabanico[1], Alexel J. Burgara-Estrella[3], Hector M. Sarabia-Sainz[4], Ana M. Guzman-Partida[5], Maria del Refugio Robles-Burgueño[5], Luz Vazquez-Moreno[5] and Jose A. Sarabia-Sainz[3✉]

[1]Departamento de Investigaciones en Polímeros y Materiales, Universidad de Sonora, Hermosillo, Sonora 83000, México; [2]Departamento de Ingeniería Química y Metalurgia, Universidad de Sonora, Hermosillo, Sonora 83000, México; [3]Departamento de Investigación en Física, Universidad de Sonora, Hermosillo, Sonora 83000, México; [4]Departamento de Ciencias del Deporte y Actividad Física, Universidad de Sonora, Hermosillo, Sonora 83000, México; [5]Laboratorio de Bioquímica y Biología Molecular de Proteínas y Glicanos, Centro de Investigaciones en Alimentos y Desarrollo, Hermosillo, Sonora 83304, México

Nanomedicine has led to the development of new biocompatible and biodegradable materials able to improve the pharmaceutical effect of bioactive components, broadening the options of treatment for several diseases, including cancer. Additionally, some snake venom toxins have been reported to present cytotoxic activity in different tumor cell lines, making them an auspicious option to be used as cancer drugs. The present study aims to evaluate the cytotoxic activity of the northern blacktailed rattlesnake (*Crotalus molossus molossus*) venom-loaded chitosan nanoparticles (Cs-Venom NPs) against the T-47D breast carcinoma cell line. To do so, we first identified the significant proteins composing the venom; afterward, hemocompatibility and cytotoxic activity against tumoral cells were evaluated. The venom was then loaded into chitosan nanoparticles through the ionotropic gelation process, obtaining particles of 415.9±21.67 nm and ζ-potential of +28.3±1.17 mV. The Cs-Venom complex delivered the venom into the breast carcinoma cells, inhibiting their viability and inducing morphological changes in the T-47D cells. These features indicate that these nanoparticles are suitable for the potential use of *C. m. molossus* venom toxins entrapped within polymer nanoparticles for the future development and research of cancer drugs.

Keywords: nanomedicine, chitosan nanoparticles, drug delivery system, rattlesnake venom, breast cancer treatment

INTRODUCTION

Nanomedicine can be defined as nanotechnology applied to health and medicine (Tran *et al.*, 2017). Hence, nanomedicine involves the use of different materials to achieve a medical benefit. Materials obtained through nanomedicine may enhance the pharmaceutical properties of bioactive agents (Tran *et al.*, 2017; Biswas *et al.*, 2012, 2014; Rizvi & Saleh, 2018; Teran-Saavedra *et al.*, 2019). The properties of these nanomaterials could prevent their rapid degradation, help target specific tissue or control its release in a stable manner (Tran *et al.*, 2017). Throughout recent years, nanomedicines have been approved by the FDA for their clinical use. Doxil™/Caelyx™ was the first nanomedicine, indicated for Kaposi's sarcoma, to be approved in 1995, and by 2016 more than 50 nanomedicines have been already approved for cancer and other pathologies (Hare *et al.*, 2017). Some nanomedicines consist of liposomal nanoparticles (Myocet™ and Doxyl™), polymeric conjugates (Oncaspar™(PEG)), polymeric micelles (Genoxol-PM™), and polymeric nanoparticles (Accurin™) (Hare *et al.*, 2017). One of the main advantages of using nanomaterials *vs.* micro or larger particles is the retention of particles smaller than 500 nm in the tumor due to the Enhanced Permeability and Retention effect (EPR) (Tran *et al.*, 2017; Hare *et al.*, 2017; Maeda, 2021; Subhan *et al.*, 2021). By encapsulating poorly soluble drugs within nanocarriers, their bioavailability may be improved and prevent their rapid clearance from the bloodstream (Tran *et al.*, 2017).

Polymers, such as albumin, PLGA (poly(lactic-co-glycolic acid)), alginate, and chitosan have been widely used as vehicles for drug transportation to different sites within an organism (Goycoolea *et al.*, 2009; Li *et al.*, 2018; Sarmento *et al.*, 2006; Gallegos-Tabanico *et al.*, 2017; Danhier *et al.*, 2012; Mir *et al.*, 2017), making them encouraging tools for drug delivery. Polymeric nanoparticles (NPs) are of particular interest due to their properties, such as the simplicity of the synthesis method, biocompatibility, and biodegradability (Calvo *et al.*, 1997; Goycoolea *et al.*, 2009; Soares *et al.*, 2018; Carreño-Gómez & Duncan, 1997).

Chitosan (Cs) is a cationic polysaccharide composed of β (1→4) linked units of *N*-acetyl-D-glucosamine and D-glucosamine (Quiñones *et al.*, 2018; Argüelles-Monal *et al.*, 2018). It is obtained by the partial deacetylation of chitin and is also naturally found in some fungi associated with other polysaccharides (Peniche *et al.*, 2008). Chitosan-based NPs have attracted scientific interest in encapsulating and delivering therapeutic biomolecules, such as drugs, genes, and proteins, among others.

Some of the nanoparticles synthesis methods include water-in-oil emulsion (Riegger et al., 2018), nanoprecipitation (Luque-Alcaraz et al., 2016), the self-assembling mechanism (Quiñones et al., 2018), and ionotropic gelation (Goycoolea et al., 2009; Calvo et al., 1997; Fernández-Quiroz et al., 2019). The latter has been used to prepare nanoparticles from polyelectrolytes in the 100–600 nm range (Goycoolea et al., 2009; Soares et al., 2018; Sawtarie et al., 2017; Wu et al., 2017) with relatively mild and straightforward procedures (Wu et al., 2017).

The possibility of using Cs for drug delivery has been thoroughly studied (Li et al., 2018a; Rampino et al., 2013; Ahmed & Aljaeid, 2016); nevertheless, few studies have been conducted with the association of animal venoms (Soares et al., 2018; Mohammadpourdounighi et al., 2010; Naser et al., 2015). The association of some animal venoms toxins and nanoparticles has been reported as an effective way to enhance therapeutical effects (Biswas et al., 2012). Additionally, snake venom toxins pose an incredible source of potential drugs for many types of diseases, including cancer (Calderon et al., 2014; Li et al., 2018).

Snake venom comprises diverse molecules, such as carbohydrates, lipids, proteins, and isoforms (Tasoulis & Isbister, 2017). Recent advances in genomics, transcriptomics, and proteomics have led to new insights regarding how they are composed. Tasoulis and Isbister reviewed the venoms of 130 different snake species and reported that 63 different protein families were generally found in them (Tasoulis & Isbister, 2017). Amongst those, four major protein families consisting of A_2 phospholipases (PLA$_2$), snake venom metalloproteinases (SVMPs), snake venom serine proteases (SVSPs), and three-finger toxins (3FTXs) (Tasoulis & Isbister, 2017). Some of these protein families are responsible for many of the clinical symptoms developed by snakebite envenomation, such as local or systemic hemorrhage, neurotoxicity, and blood clotting anomalies (Masuda et al., 1998; Torii et al., 1997; Suhr & Kim, 1996; Meléndez-Martínez et al., 2017; Chellapandi, 2014; Park et al., 2009; Bénard-Valle et al., 2014; Calderon et al., 2014; Calvete et al., 2009). Interestingly enough, several studies have reported that some of these toxin families have cytotoxic action against tumoral cells (Calderon et al., 2014; Li et al., 2018b; Hayashi et al., 2012; Kerkis et al., 2014; Lee et al., 2016; Marinovic et al., 2017; Azevedo et al., 2016). Given the biological mechanisms by which they interact with different tissues, cells, and receptors, snake venom toxins can induce apoptosis, inhibit angiogenesis, tumoral growth, and cell migration (Biswas et al., 2012; Calderon et al., 2014; Al-Sadoon et al., 2013; Badr et al., 2013). Additionally, it has been reported that the interaction of some of these toxins with nanoparticles may enhance their therapeutical effects (Gláucia-Silva et al., 2018; Soares et al., 2018; Agarwal et al., 2019; Karpel et al., 2018; H & N, 2009; Biswas et al., 2012).

The purpose of the present study was to characterize the venom of a northern black-tailed rattlesnake (C. m. molossus) for protein identification and evaluate it for hemocompatibility in human red blood cells and cytotoxic activity in the T-47D breast carcinoma cell line. Additionally, chitosan nanoparticles were prepared as a matrix to evaluate their ability to entrap the rattlesnake venom, their hemocompatibility, and evaluate if the cytotoxic activity presented in the tumoral cell line stayed unhinged.

MATERIALS AND METHODS

Materials

All the reagents used were analytical grade and, unless specified, purchased from Sigma-Aldrich (St. Louis, MO, USA). Low molecular weight chitosan (Cs, Sigma-Aldrich; the degree of deacetylation was certified by the supplier as ~76%, with an $\overline{M}_v$ of ~95 kDa), pentasodic tripolyphosphate (≥98%) (TPP), sodium chloride (≥99%) (NaCl), Glycerol (≥99%), bovine serum albumin (66.5 kDa and ~96%) (BSA), Dulbecco's Modified Eagle Medium (DMEM), fetal bovine serum (FBS), and [3-5-dimethylthiazol-2-yl]-2, 5-diphenyltetrazolium bromide (MTT). T-47D cells were obtained from the ATCC (American Type Culture Collection, Manassas, VA, USA). All the experiments were carried out using Type 2 ultrapure water (0.18 μS/cm).

Ethics Statement

The Research Ethics Committee approved the present study of the Universidad de Sonora. Experiments comply with the principles expressed in the declaration of Helsinki. Blood was drawn from participants who signed informed consent and agreed for their blood to be used in hemolysis assays.

C. m. molossus Venom Extraction

Venom extraction was performed at the Itinerant Wildlife Museum (MIVIA) following the American Society of Ichthyologists and Herpetologists guidelines for the use of live amphibians and reptiles were followed. Secretariat of Agriculture and Livestock (SAGARHPA) issued captive animals, and venom extraction for scientific purposes permit numbers 12/09-00462/15 and DGFF/12/09-1106/18.

Three male adult snakes from the scientific collection of the MIVIA in Hermosillo, Sonora, Mexico, were used for venom extraction. Venom was extracted manually by allowing the snakes to bite sterile 100 mL plastic containers covered with parafilm, obtaining an average of 800 μL per extraction. Afterward, venom was stored at –80°C for 24 h and then lyophilized. For use, the lyophilized venom was resuspended in ultrapure water and centrifuged at 2000×g for 15 minutes for debris removal.

Protein Concentration

The protein concentration of the venom samples and the encapsulation efficiency (EE%) were determined with slight modifications by the Bradford microplate protein quantification method (Bradford). Briefly, different samples of known concentrations of BSA were prepared (1:10, BSA sample: Bradford reagent), and absorption (ABS) was read in a UV-spectrophotometer at 595 nm to obtain a protein calibration curve and equation (Thermo Scientific Multiskan GO). Afterward, samples from C. m. molossus venom were quantified by measuring the ABS of the supernatant and comparing the values with the calibration curve previously obtained.

Venom Characterization

SDS-PAGE. Proteins from the venom were analyzed by electrophoresis using reducing and denaturalizing conditions (SDS-PAGE) in a 15% polyacrylamide gel according to Laemmli (Laemmli, 1970). PAGE analysis was done using 10 μg of venom protein and subsequent-

ly stained with Coomassie. The molecular weight of the proteins was estimated by comparing them to broad-range molecular weight markers (Bio-Rad, Hercules, CA, USA).

Protein Digestion and Liquid Chromatography-Tandem Mass Spectrometry Analysis (LC-MS/MS). The three electrophoretic protein bands with the highest intensity were excised from the gel, reduced with 10 mM DTT in 25 mM ammonium bicarbonate, and subsequently alkylated with 55mM iodoacetamide, according to a procedure described by Huerta-Ocampo and others (Huerta-Ocampo *et al.*, 2014). Protein digestion was carried out overnight at 37°C with sequencing-grade trypsin (Promega, Madison, WI, USA). Tryptic peptides were dried by centrifugation in a vacuum, suspended in 0.1% trifluoroacetic acid, and purified using ZipTip (Merck Millipore, Darmstadt, Germany).

Trypsinized peptides were subjected to reverse-phase ultraperformance liquid chromatography using the 1290 Infinity LC System (Agilent Technologies, Santa Clara, CA, USA) associated with an analytical column ZORBAX 300SB-C8 (5 μm×2.1 mm×150 mm, Agilent Technologies, Santa Clara, CA, USA), coupled to a Dual AJS ESI ionization source (Agilent Technologies, Santa Clara, CA, USA). Afterward, they were analyzed by tandem mass spectrometry through a data-dependent analysis in the 6530 Accurate-Mass Quadrupole Time-of-Flight (Q-TOF) LC/MS system (Agilent Technologies, Santa Clara, CA, USA) with the chromatographic and MS/MS conditions (Morales-Amparano *et al.*, 2019) using Agilent MassHunter Workstation Software package (Agilent Technologies, Santa Clara, CA).

Protein Identification. The MS/MS raw data of the tryptic digests from the electrophoretic bands were interpreted to determine protein identities and relative abundances using a Spectrum Mill MS Proteomics Workbench software package (Agilent Technologies, Santa Clara, CA), also using PA *Crotalus* + cont.fasta in-home database. Search parameters included carbamidomethylation of cysteines as fixed modification, methionine oxidation as variable modification, 50% minimum matched peak intensity, individual ion scores ≥12, and scored peak intensity (SPI) ≥60 were considered as suitable matches. In contrast, protein score ≥25 and at least two peptides were necessary for confident protein identification. In addition, the MS/MS raw data were converted to .mgf files in the MassHunter Workstation Software Qualitative Analysis and processed in search engine MASCOT free version. The using search parameters including carbamidomethylation of cysteines as fixed modification, methionine oxidation as variable modification, 50% minimum matched peak intensity, 20 ppm and 0.1 Da on precursor tolerance and production masses, respectively, 1 missed tryptic cleavage, and ESI-Q-TOF scoring parameters.

Hemolytic Activity Assays

The Research Ethics Committee approved the present study of the Universidad de Sonora. Experiments comply with the principles expressed in the declaration of Helsinki. Blood was drawn from participants who signed informed consent and agreed for their blood to be used in hemolysis assays. Experiments were performed as described by Diaz-Galvez and others (Diaz-Galvez *et al.*, 2019), with slight modifications. Briefly, these blood samples were drawn and then transferred to clean tubes (BD Vacutainer EDTA anticoagulant); afterward, 15 μL of blood were diluted in 1 mL of PBS. Then, 0.046–

3 mg/mL of snake venom samples were incubated at 37°C for 24 h and then centrifuged at 2000×g×1 minute. Hemolysis was determined by the absorbance of the supernatant at 540 nm, using a spectrophotometer (Thermo Scientific Multiskan GO). Blood diluted in PBS was used as a negative control for hemolysis, and blood diluted in water was used as a positive control. For the Cs NPs, the same procedure was followed, but instead of using *C. m. molossus* venom, concentrations ranging from 0.0046–3 mg/mL of Cs-Blank and Cs-Venom NPs were evaluated.

Cell Viability Assays

The Research Ethics Committee approved the present study of the Universidad de Sonora. Experiments comply with the principles expressed in the declaration of Helsinki. Cell viability assays were performed in the T-47D breast carcinoma cell line, using [3-5-dimethyl-thiazol-2-yl]-2, 5-diphenyltetrazolium bromide (MTT) (Diaz-Galvez *et al.*, 2019). Briefly, cells were seeded in 48-well plates at a density of 10 000 cells/200 μL per well using DMEM containing 10% FBS. Cells were incubated at 37°C and 5% CO_2 for 24 h. Afterward, the medium was replaced for 0.98–31.25 μg/mL of venom in DMEM for 24 h. The Cytotoxic Concentration$_{50}$ (IC_{50}) value of the venom in the T-47D breast carcinoma cells was thus determined. For the Cs NPs, the same procedure was followed, but instead of using *C. m. molossus* venom, concentrations ranging from 0.98–31.25 μg/mL of Cs-Blank and Cs-Venom NPs were evaluated.

Venom-loaded Nanoparticle Synthesis

The preparation of Cs NPs was done similarly to what Calvo and others (Calvo *et al.*, 1997) described, with slight modifications. Briefly, chitosan (Cs) was dissolved (2 mg/mL) in 1% acetic (v/v). Afterward, NaCl (0.4% w/v) was added to the Cs solution and stirred for 15 min. A mixture of TPP (4 mg/mL) and snake venom (5 mg/mL) was prepared for the crosslinker solution. Then, the TPP-Venom solution was added dropwise (10:1, Cs: crosslinker solution) to form the Cs-Venom NPs spontaneously.

For blank NPs, the same procedure was done but without adding *C. m. molossus* venom in the TPP solution. Nanoparticles were isolated by centrifugation (13 000 rpm for 30 min at 4°C) using a bed of glycerol (20 μL) at the bottom of the vial. The supernatant was carefully removed, and the pellet was resuspended in water for characterization. The venom's encapsulation efficiency (EE%) was determined by the Bradford method; the supernatants of the particles obtained through the isolation process were quantified following the same procedure described in section 2.4. The EE% calculation was determined with equation (1).

$$EE\% = \frac{Total\ protein - Supernatant\ protein}{total\ protein} \times 100$$

Nanoparticle Characterization

Dynamic Light Scattering and ζ-Potential. The particle size (mean particle diameters and size distributions) and ζ-potential of NPs were measured at 25°C using dynamic light scattering (DLS) at a scattering angle of 90° with Zetasizer Nano ZS90 (Malvern Instruments Ltd, Malvern UK) with a doppler anemometry laser. Samples were diluted in water (0.5:1 mL). All the measurements were done in triplicate.

Fourier Transformed Infrared Spectroscopy. The structural characterization of these nanomaterials was performed by infrared spectra using Agilent Cary 630 FTIR Spectrometer (Agilent, Cary 630 FTIR Spectrometer, Santa Clara, CA, USA) a resolution of 4 cm^{-1} in the range of 650 to 4000 cm^{-1} in ATR mode.

Nanoparticle Morphology. The morphology of NPs was characterized by atomic force microscopy (AFM, Alpha 300RA, WiTec, Germany). AFM images were reconstructed in the non-contact mode using nanosensors with a spring constant of 42 N/m and a resonant frequency of 285 kHz. The analyses were performed using 5×5 μm scanning images with WiTec project FOUR v4.1 software.

Fluorescence Intensity of Rhodamine 123

T-47D cells were seeded in 48-well plates at a density of 10 000 cells/200 μL per well using DMEM containing 10% FBS. After incubation (37°C and 5% CO$_2$ for 24 h) cells were washed three times with 200 μL of physiological saline solution (PSS). Subsequently, the cells were incubated with PBS containing venom from *C. m. molossus* and NPs (Cs-Blank and Cs-Venom) at a 7.81–31.25 μL/mL at 37°C for 30 min. Then, they were rinsed three times again with PSS (200 μL). The fluorescence intensity (FI) was measured as follows: the cells were stained with 1 μg/mL of rhodamine 123 and incubated for 15 min at 37°C. Finally, fluorescence and cell morphology were analyzed under confocal microscopy (Nikon TiEclipse C2+, Japan) with 488 nm lasers. Images were obtained with a 1024×1024 pixels resolution and 20× magnification and analyzed by imaging software NIS-Element.

Statistical Analysis

Two-way ANOVA followed by Sidak's and Tukey's multiple comparison tests were performed in GraphPad Prism 8.0.2 for Windows (GraphPad Software, San Diego, California, USA, www.graphpad.com). *P* values≤0.005 were considered significantly different.

RESULTS AND DISCUSSION

Venom Characterization

When using snake venom, it is imperative to know what toxins or toxin families compose it, which helps to
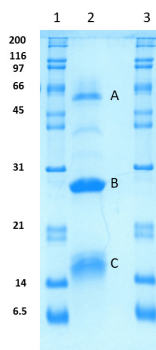
Figure 1. 15% SDS-PAGE gel electrophoresis of *C. m. molossus* venom from Hermosillo, Sonora, Mexico under reducing conditions.
Different bands with molecular masses of ~65 kDa, 23 kDa, and 16 kDa (**A**, **B**, and **C**, respectively) were separated from the venom. LC-MS/MS analysis identified these bands as a P-III SVMP and LAAO (band A), a P-I SVMP (band B), and a PLA$_2$ (band C). 10 μg of venom were loaded in lane 2.

discuss the possible outcomes of any performed analysis and facilitate any experiment replications. Electrophoresis gel analysis was performed in reducing conditions to separate the protein bands in the black-tailed rattlesnake, *C. m. molossus*, venom. Proteins migrated with relative molecular mass from ~65 kDa to ~16 kDa. Three major protein bands A, B, and C (Fig. 1) were selected for further analysis.

Intraspecific venom variation has been previously reported for several species of rattlesnakes (Borja *et al.*, 2018; Castro *et al.*, 2013; Tasoulis & Isbister, 2017). The presence of molecular weights in the 50–75 kDa and 20–25 kDa, as well as the absence of molecular weights under ~10 kDa, are similar to the adult Mexican black-tailed rattlesnake (*C. m. nigriscens*) venom reported by Borja and others (Borja *et al.*, 2018).

Additionally, the three main protein bands (A, B, and C) were analyzed by LC-MS/MS. Table 1 shows the two identified proteins by MS/MS spectra analysis of the tryptic digest of band A using two search engines (Spectrum Mill and Mascot). These proteins were the Zinc disintegrin-like metalloproteinase (VAP2A) that belongs to the P-III SVMPs toxin family. Also, this band contained more than one protein, L-amino acid oxidase (Apoxin I) was also identified. SVMP HT-2 metalloproteinase that belongs to the P-I SVMPs toxin family with a relative mass of ~30 kDa was identified in the band B. Lastly, a Phospholipase A2_2 with a relative mass of ~16 kDa was identified in band C. Borja *et al.* reported that the venoms of 20/27 of the studied specimens of *C. m. nigriscens* presented bands with a similar mass to that of the identified PLA$_2$ (Borja *et al.*, 2018).

In previous reports, it has been found that some of the toxin families found in the *C. m. molossus* venom, like SVMPs and PLA$_2$s, have cytotoxic effects in different tumoral cell lines (Calderon *et al.*, 2014; Tang *et al.*, 2004; Boldrini-França *et al.*, 2020; Marinovic *et al.*, 2017; Du & Clemetson, 2002; Rivas-Mercado & Garza-Ocañas, 2017). A P-III snake venom metalloproteinase (SVMP) was identified in band A figure 1; this band may contain another protein. VAP2A, also known as vascular apoptosis-inducing protein 2A, is a P-III type SVMP first described by Masuda and others (Masuda *et al.*, 1998). It can induce apoptosis in vascular endothelial tissue (Masuda *et al.*, 1998). It has been previously proposed a possible therapeutic use for this toxin due to its properties to inhibit angiogenesis, a vital process for tumoral cell growth (Masuda *et al.*, 1998). SVMPs usually cause hemorrhagic symptoms in clinical patients through blood coagulation changes or interaction with the extracellular matrix (ECM) components, such as collagen, laminin, and fibronectin (Calderon *et al.*, 2014). The formation of new blood vessels has been reported with the action of matrix metalloproteases/ADAM proteins and in cell-cell/cell-ECM adhesion (Calderon *et al.*, 2014). Thus, the action of SVMPs takes an exciting role in the possible antitumoral effect by inhibiting tumoral growth, as well as tumoral adhesion. The latter is because some SVMPs have been reported to interact with important receptors that mediate metastasis and cell migration (Calderon *et al.*, 2014; Arvelo & Cotte, 2006; Kamiguti *et al.*, 1998; Gutiérrez & Rucavado, 2000). The similarity that the SVMPs and mammalian matrix metalloproteinases (MMPs) have opens the possibility that these snake venom toxins may be used as potential therapeutic targets or agents against cancer (Calderon *et al.*, 2014; Tang *et al.*, 2004; Alaseem *et al.*, 2019).

Apoxin I is an L-amino acid oxidase (LAAO), was also identified in band A Fig. 1. Apoxin I has been de-

Table 1. Venomic analysis of the *C. m. molossus* venom through Liquid Chromatography-Tandem Mass Spectrometry (LC-MS/MS).

Electrophoretic band	ID Code (UniProt)	Organism	Protein	Toxin Family	Molecular mass (kDa)
A	A4PBQ9	Crotalus atrox	Zinc disintegrin-like metalloproteinase (VA-P2A)	P-III SVMP	65.854
	P56742	Crotalus atrox	L-aminoacid oxidase (Apoxin I)	LAAO	56.737
B	P20897	Crotalus ruber	SVMP HT-2 metalloproteinase (Ruberlysin)	P-I SVMP	23.321
C	ANN23923	Crotalus molossus	Phospholipase A$_2$ (Phospholipase A2_2)	PLA$_2$	16.251

scribed as an apoptosis-inducing factor, considered one of the causes of hemorrhagic symptoms in rattlesnake-bite patients (Torii *et al.*, 1997). Several biological effects have been attributed to the action of this toxin, such as edematogenic processes, hemolysis, antibacterial and antiparasitic activity, and regulation of platelet aggregation (Torii *et al.*, 1997, 2000). Although the LAAOs mechanisms' have not been fully comprehended, it has been hypothesized that their interaction with different cell receptors can increase hydrogen peroxidase (H$_2$O$_2$) levels in cell membranes. High peroxidase levels due to oxidative processes may induce apoptosis in different cell lines, such as human embryonic cells (293T), human promyelocytic leukemia cells (HL-60), rat lymphocytic leukemia cells (L1210), and human leukemia cells (Torii *et al.*, 1997; Calderon *et al.*, 2014; Zhang *et al.*, 2003; Samel *et al.*, 2006; Suhr & Kim, 1996). Apoptosis induction from this toxin is a polemic one within the scientific community. Although it has been reported that it is related to the rise in peroxide levels, reports have shown that it is not the only reason (Calderon *et al.*, 2014; Suhr & Kim, 1996; DiPietrantonio *et al.*, 1999) and thus, further research is necessary.

Ruberlysin, a P-I SVMP, was identified in band B figure 1. It has been reported that ruberlysin induces local hemorrhages by acting within blood vessels' inner walls (Takeya *et al.*, 1990). As has been mentioned before, SVMPs can interfere with components in the ECM (Calderon *et al.*, 2014). Ebrahimian evaluated its capacity to induce apoptosis in Neuro-2a, neuroblastoma cell line, alongside other toxins from the red diamondback rattlesnake (*Crotalus ruber*) (Ebrahimian, 2013).

Finally, A2_2 phospholipase was identified in band C figure 1, as its name suggests it is an A$_2$ type phospholipase (PLA$_2$). PLA$_2$s have a wide diversity of biological effects, such as inducing neurotoxicity and myotoxicity and play essential roles in lipid metabolism (Calderon *et al.*, 2014). PLA$_2$s activity is highly related to the metabolism of cell membranes. Different types of PLA$_2$s, such as basic and acidic, have shown antitumoral and antiangiogenic activity *in vitro* and *in vivo*, suggesting a new approach for developing antitumoral agents (Calderon *et al.*, 2014). Modahl and Mackessy (Modahl & Mackessy, 2016) described in their extensive study that the *C. molossus* venom presented three different isoforms of PLA$_2$s. Amongst those different isoforms, they reported sequences belonging to neurotoxic and myotoxic PLA$_2$s. For example, Crotoxin B is a ~14 kDa PLA$_2$ neurotoxin that binds and activates cell receptors in the cell membrane, thus interfering with the epidermal growth factor, inhibiting tumoral growth (Calderon *et al.*, 2014; Corin *et al.*, 1993). Borja and others (Borja *et al.*, 2018) reported more presence of crotamine-like toxins in the venom from young Mexican black-tailed rattlesnakes, *C. m. nigriscens* (Borja *et al.*, 2018). These crotamine-like toxins had an average molecular mass of ~10 kDa (Borja *et al.*, 2018a). In our study, the smallest toxin observed in the

electrophoretic gel had a relative mass of ~16 kDa, associated with PLA$_2$s. In this case, more studies and research are needed for the complete profiling of the *C. m. molossus* in the northwestern region.

Hemolytic Activity of *C. m. molossus* venom. The red blood cells (RBCs) are the most abundant in the blood and are in continuous contact with exogenous compounds; therefore, the HA of the venom of *C. m. molossus* was evaluated. Values obtained below 10% hemolysis can be considered non-hemolytic, while those equal to or higher to 25% are hemolytic (Amin & Dannenfelser, 2006). The snake venom was slightly hemolytic at the higher concentrations evaluated (0.75–3 mg/mL) and non-hemolytic below those (Fig. 2). Water-treated RBCs were used as the positive control and PBS as the negative one for hemolysis.

Some of the clinical symptoms of rattlesnake bite envenomation include proteolytic activity such as fibrinolysis, hemolysis, or platelet aggregation (Meléndez-Martínez *et al.*, 2017). As observed in the black-tailed rattlesnake venom HA assay (Fig. 2), *C. m. molossus* venom was not hemolytic at concentrations below 0.75 mg/mL. Contrary to what we observed, Macías-Rodríguez and others (Macias-Rodríguez *et al.*, 2014) compared the HA of the venom of two subspecies of *C. molossus*, *C. m. nigriscens* and *C. m. molossus*, and reported that both presented HA. Borja and others (Borja *et al.*, 2018a) reported ontogenetic differences in the venom composition of *C. m. nigriscens*, where juvenile specimens had a more neurotoxic-like venom, and adults had a more hemorrhagic-like one. The snakes used in this study were adults, and it is noteworthy to consider the last since different ages between these snakes could provide different venom copositions,
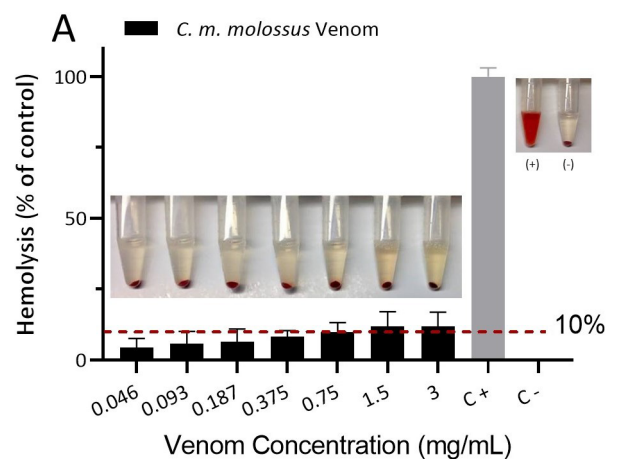
Figure 2. Hemolytic activity (HA) of the *C. m. molossus* venom. Lower tested concentrations of the venom were slightly hemolytic, while higher ones tested were hemolytic. Water treated RBCs were used as the positive control; data represents means and ± standard deviation from triplicates.
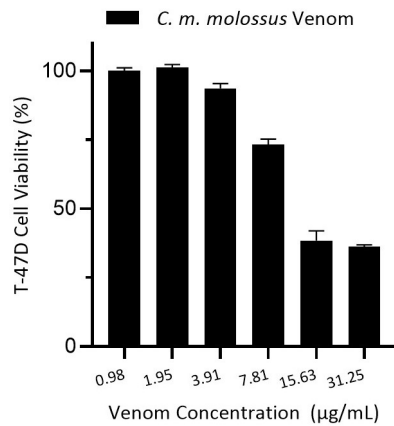
Figure 3. MTT cell viability assay was performed with different concentrations of *C. m. molossus* venom.
An IC_{50} value of 15.45 µg/mL was determined. Cell viability was lowered by >60% at 31.25 µg/mL; data represents means and ± standard deviation from triplicates.

thus, different results in these types of assays. Thus, having a < 0.75 mg/mL venom concentration could help avoid the HA observed at higher concentrations. Additionally, the black-tailed rattlesnake venom was evaluated for cytotoxic activity against the T-47D breast carcinoma cell line.

***C. m. molossus* Venom Tumoral Cytotoxic Activity.** MTT assays were performed to determine the cytotoxic activity of the black-tailed rattlesnake venom in the T-47D breast carcinoma cell line. We observed a significant diminish of T-47D cells viability provoked by the snake venom toxins (Fig. 3). The IC_{50} of the venom was 15.45±0.93 µg/mL. As expected, the lowest tumoral cell viability, ~36 %, was observed at the highest venom concentration used, 31.25 µg/mL, well below the HA concentrations shown in figure 2. Thus, we confirmed that the venom of the black-tailed rattlesnake (*C. m. molossus*) presents cytotoxic activity in the T-47D breast carcinoma cell line.

Tasoulis and Isbister (Tasoulis & Isbister, 2017) reviewed different snake venoms contents from the world's prominent medically necessary snake families. They concluded that three main toxin families (SVMPs, SVSPs, and PLA$_{2}$s) are found in the Viperinae snake sub-family venoms, where the genus *Crotalus* is located. Meléndrez-Martínez and others (Meléndez-Martínez et al., 2017) reported that *C. molossus* venom contained several different toxin families, including the aforementioned. In their review, Calderon and others (Calderon et al., 2014) described the different mechanisms by which many snake venom toxins present tumoral cytotoxic effects. A lower T-47D breast carcinoma cell viability was observed at higher concentrations of *C. m. molossus* venom. Our study shows an IC_{50} value of 15.45 µg/mL (Fig. 3). Different venom compositions could change the outcome of these types of tests, and said compositional changes might happen due to ontogenetic changes (Borja et al., 2018a), geographical range (Borja et al., 2018a; Borja et al., 2018b) and, not as common as the aforementioned, sex (Borja et al., 2018a; Furtado et al., 2006).

Considering the identified toxins (Table 1), we infer that the cytotoxic activity observed in the MTT assays is due to the action of the different SVMPs, LAAO and PLA$_2$ found. As mentioned before, SVMPs can interact with components of the ECM and produce apoptosis in vascular endothelial cells (Masuda et al., 1998; Calderon et al., 2014; Takeya et al., 1990; Chellapandi,

2014), thus, inhibiting tumoral proliferation and reducing angiogenesis. On the other hand, LAAOs have been reported to produce high concentrations of H_2O_2, hydrogen peroxide by interacting with different cell membrane receptors (Calderon et al., 2014; Torii et al., 1997). LAAOs from different rattlesnake species like *C. adamanteus* and *C. atrox* have been reported to act specifically with mammalian endothelial cells (Calderon et al., 2014; Suhr & Kim, 1996; Du & Clemetson, 2002) as it was mentioned above. PLA$_2$s have been reported with antitumoral and antiangiogenic activity. Commonly, their interactions with different cell membrane receptors in membrane lipids have shown inhibition in tumoral growth and cell adhesion (Calderon et al., 2014; Chwetzoff et al., 1989). Additionally, the observed IC_{50} of the snake venom was 15.45±0.93 µg/mL, a much lower concentration than that of the recommended use in section 3.1.2. More studies are required to observe how these toxins interact with the T-47D breast carcinoma cells. Once the venom was characterized and evaluated, venom-loaded polymeric nanoparticles were obtained and evaluated.

Cs-Venom Nanoparticles

In this research, the black-tailed rattlesnake venom was entrapped into a Cs nanoparticle system using TPP as a crosslinking agent by ionotropic gelation.

Formation of Nanoparticles. Cs-Venom NPs were obtained spontaneously by the addition of the TPP-Venom solution to the Cs solution. It is known that the mechanism of Cs-TPP ionotropic gelation is driven by the process of intra- and intermolecular linkages, which is promoted by amine groups of chitosan and the negatively charged species of TPP (Calvo et al., 1997; Pedroso-Santana & Fleitas-Salazar, 2020; Rampino et al., 2013; Fernández-Quiroz et al., 2019).

Results for different formulations are shown in Table 2. Cs-Blank NPs were obtained with a hydrodynamic size (D_H) of 506 nm. These values are slightly higher than those reported for similar nanoparticle systems (Goycoolea et al., 2009). These results may be due to the molecular characteristics of the polysaccharides, such as molecular weight and degree of deacetylation of Cs.

Table 2. Different formulations of Cs NPs with and without venom.

	Cs-Blank NPs	Cs-Venom NPs
D_H (nm)	506.4±14.05	415.9±21.67
PDI	0.47±0.01	0.44±0.03
ζ-potential	27.3±1.65	28.3±1.17

Data are means and ± standard deviation for triplicate.

Cs-Venom NPs exhibited a positive ζ-potential, which suggests the presence of a shell of chitosan in the formulations. The formulation exhibited a D_H of ~415 nm and a ζ-potential of ~28 mV (Table 2). The decrease in the size of venom-loaded NPs concerning the blank NPs is shown. The electrostatic forces between the venom extract and chitosan are the dominant interaction in this system. The venom extract used for the preparation of nanoparticles may provide the presence of a polypeptide mixture, which may lead to additional intra- or inter-molecular interactions. Hence the decrease in particle size.

The encapsulation efficiency (EE%) of the venom entrapped in the Cs-Venom-NPs was determined
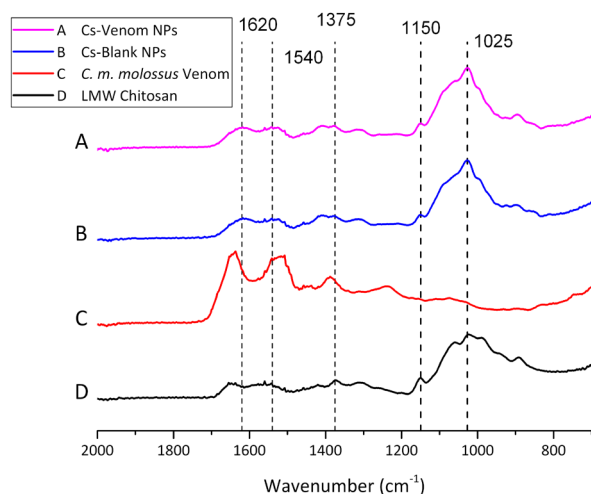
Figure 4. FTIR analysis of venom-loaded (A) and blank (B) NPs, as well as their main individual components, (C) *C. m. molossus* venom, (D) LMW Chitosan.

through a Bradford protein stain microplate protocol. The EE% was 48.29±3.84%. Soares and others (Soares *et al.*, 2018) entrapped the snake venom of two different viperids, *Bothrops erythromelas* and *B. jararaca*, achieving an EE% of over 65% of both venoms with a Cs-TPP NP system. Goycoolea and others (Goycoolea *et al.*, 2009) were able to achieve an EE% of up to 41–52% for insulin, using a hybrid Cs-ALG NP system, they suggested that the electrostatic interactions given between the Cs and insulin were the most dominant, nevertheless, other interactions should also be considered.

ATR-FTIR Analysis. FTIR analysis was performed to evaluate the molecular composition of the obtained products. Figure 4 shows the spectra of Cs-Venom NPs (A) as well as Cs-Blank NPs (B) and their main individual components, *C. m. molossus* venom (C) and LMW Cs (D). There are apparent differences between the spectra obtained from the NPs and their main individual components. The signals observed at 1540 cm^{-1} and 1620 cm^{-1} in the venom-loaded and blank NPs (A and B) spectra correspond to the Amide I and Amide II bands of chitosan (Soares *et al.*, 2018), respectively. A slight shift from a small peak at 1640 cm^{-1} from LMW chitosan (D) to 1620 cm^{-1} (A and B) is observed. Additionally, LMW chitosan and both NPs show the characteristic 1375 cm^{-1}

corresponding to -CH$_3$ symmetrical deformation vibration of chitosan.

Soares and others (Soares *et al.*, 2018) reported the FTIR spectra of Cs-TPP NPs entrapping the snake venom of *B. erythromelas* and *B. jararaca*. They mentioned how the interaction between the NP components and the snake venom might result in band shifts and separation of the absorption bands. They observed a shift in the C=O primary (1540 cm^{-1}) and secondary (1640 cm^{-1}) protein bands. In contrast with our results, there was no apparent shift in said bands (A and B), but a slight shift from 1640 cm^{-1} to 1620 cm^{-1} is noticed. Additionally, the peaks corresponding to the C-N stretches of chitosan's primary and secondary amines can be observed at 1025 cm^{-1} and 1150 cm^{-1}, respectively, in A, B, and D (Coates, 2000). These results confirm the Cs-TPP conjugation (Mohammadpourdounighi *et al.*, 2010). There was no difference between the spectra of blank and venom-loaded NPs (A and B) in our study. The last could be attributed to the relatively low penetration capacity of the ATR mode used. There are noticeable differences between the pristine components (C) and the obtained NPs (A and B).

NPs Morphology. The morphology of the venom-loaded and blank NPs was observed through atomic force microscopy (AFM) (Fig. 5). Figure 5A, Cs-Blank NPs presented a smooth surface, semi-spherical shape, and ~500 nm of size. Similarly, in Figure 5B, Cs-Venom NPS showed a smooth surface, a semi-spherical shape, and an estimated size of ~400 nm.

Similar to other studies that also entrapped snake venom within Cs NPs, our venom-loaded NPs presented a smooth surface and semi-spherical shaped morphology (Fig. 5 A and B) (Soares *et al.*, 2018). Naser and others (Naser *et al.*, 2015) observed that the interaction of scorpion venom with the Cs chains could increase the NP size, although no increase in size was observed with our NPs, as confirmed by the DLS data in Table 2.
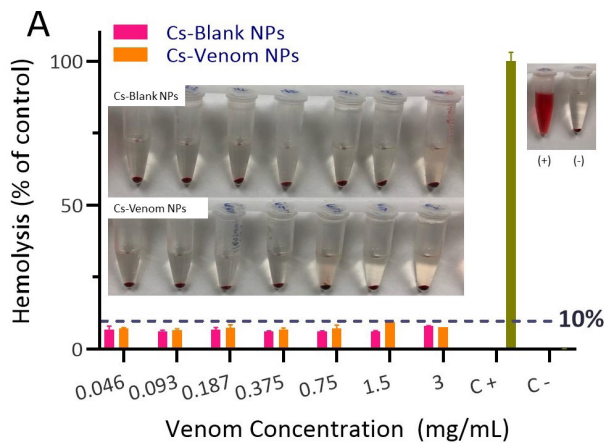
Hemolytic Activity of Venom-loaded NPs

HA assays were performed with Cs-Venom NPs to study their behavior with RBC. It can be observed (Fig. 6) that, similarly to the HA observed in Fig. 2, the higher concentrations (0.75–3 mg/mL) were slightly hemolytic, whereas the lower ones were not. The entrapment of the venom within the Cs matrix may protect the RBCs; hence, further studies are required.

Zhou and others (Zhou *et al.*, 2015) studied the hemocompatibility of Cs dendrimers and Cs alone, and they reported that at 50 and 100 µg/mL, the Cs dendrimers induced higher hemolysis than Cs alone. Their study

A. Cs-Blank NPs
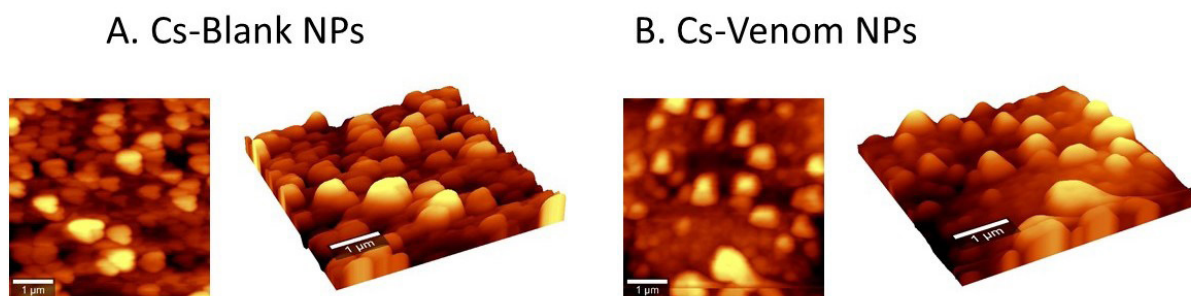
B. Cs-Venom NPs

Figure 5. 2D and 3D AFM images of blank and venom-loaded NPs.

Figure 6. Hemolytic activity (HA) venom-loaded and blank NPs.
Cs-Venom NPs were not hemolytic, specially at lower concentrations <0.187 mg/mL. PBS and water were used as (–) and (+) control, respectively.
Data are means and ± standard deviation for triplicate.

reported a 2%<HA<5% indicating that they were non-hemolytic. In the present work, the results show that the Cs-Venom NPs were slightly hemolytic (HA>10%) at high concentrations (Fig. 6). In the same way, the Cs-Blank NPs were slightly hemolytic (HA>10%) at high concentrations (Fig. 6). The venom from the black-tailed rattlesnake, *C. molossus*, has been previously reported as more hemolytic than the western diamondback rattlesnake, *C. atrox*, or the tiger rattlesnake, *C. tigris*, due to its capacity to degrade fibrinogens and collagen (Meléndez-Martínez *et al.*, 2017). Although the venom of *C. molossus* has been previously studied, even more studies are required to establish isolated toxins or whole venom to be used as possible pharmaceutical agents. Although the venom-loaded NPs have toxins that may interact with RBC membranes or components of the ECM, there was not enough decrease in the RBC viability to be labeled as hemolytic (HA>10%). Hence, the latter suggests that
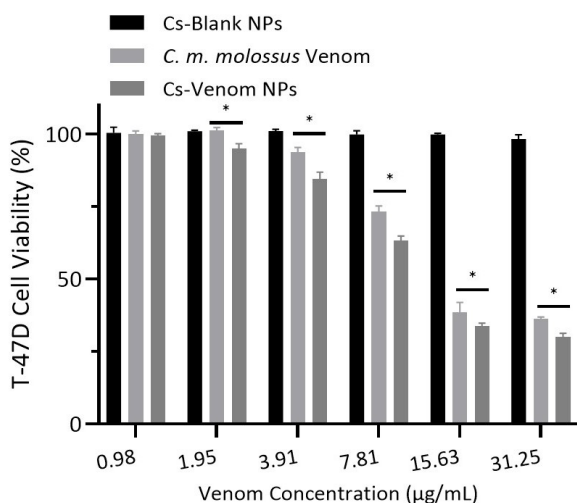
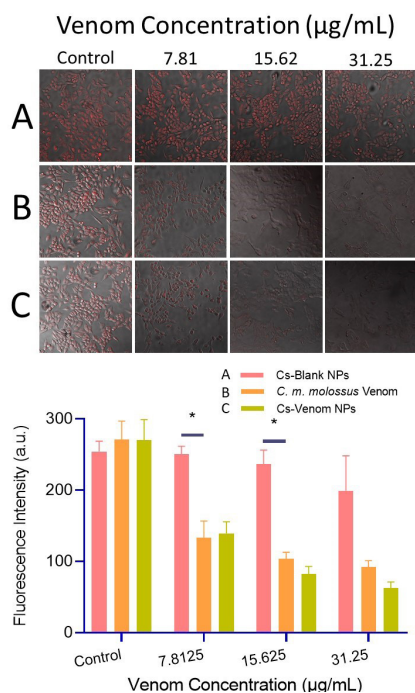the evaluated concentrations of NPs formulations do not produce hemolysis.

Venom-Loaded NPs Tumor Cytotoxic Activity.

The tumoral cytotoxic activity was analyzed through MTT assays. As observed (Fig. 7), the Cs-Venom NPs inhibit the cell viability, down to ~30%. Additionally, the Cs-Blank NPs did not inhibit the cell viability of the T-47D breast carcinoma cell line. Significant differences were found between the snake venom *vs.* Cs-Venom NPs' cytotoxic effect in a 2-way ANOVA followed by Sidak's multiple comparison test.

Cs has been firmly established as a biocompatible and low toxic polymer (Calvo *et al.*, 1997; Goycoolea *et al.*, 2009; Soares *et al.*, 2018; Wu *et al.*, 2017); nevertheless, Carreño-Gómez and Duncan (Carreño-Gómez & Duncan, 1997) reported cytotoxic activity of different Cs salts, being time and exposed concentration the most important factors for it. In another study by Zaki and others (Omar Zaki *et al.*, 2015), it was reported that for Cs-TPP NPs, size and concentrations were determinant factors in the obtention of cytotoxic activity *in vitro*. Our results show, as expected, no apparent cytotoxic activity from the Cs-Blank NPs, having average cell viability of 100.08±0.99% for all analyzed concentrations. The Cs-Venom NPs could decrease the cell viability of the T-47D breast carcinoma cell line (Fig. 7). A decrease to 30.03±1.27% viability was obtained at the highest Cs-Venom NP concentration (31.25 µg/mL). It is noteworthy that all the concentrations used with the Cs-Venom NPs were significantly different and lower than the cell viability obtained by the whole venom. The last indicates a possible potentiating effect of the polymer matrix, similar to what was reported for other pharmaceuticals (Tran *et al.*, 2017; Aftab *et al.*, 2018). Biswas and others (Biswas *et al.*, 2012) and Al-Sadoon and others (Al-Sadoon *et al.*, 2013) had already reported the possible use of combined nanostructure alongside snake venom for pharmaceutical use. As reported elsewhere, the toxins herein identified (SVMPs, LAAO, and PLA$_2$) have been previously described as potential pharmaceutical agents, inhibiting tumoral growth and inducing apoptosis (Calderon *et al.*, 2014; Suhr & Kim, 1996; Chellapandi, 2014; Al-Sadoon *et al.*, 2013; Badr *et al.*, 2013; Park *et al.*, 2009). Our results indicate a potentiating effect of the snake venom entrapped within the Cs NPs, hence lower cell viability. As indicated before, snake venoms have been reported as exciting and promising tools for pharmaceutical research (Calderon *et al.*, 2014; Park *et al.*, 2009; Azevedo *et al.*, 2016; Chwetzoff *et al.*, 1989; Mohammadpourdounighi *et al.*, 2010), and, we were also able to confirm that the cytotoxic effect was produced by the entrapped venom and not the Cs NPs by themselves (Fig. 7). More studies are required to confirm any possible effect between the proteins encapsulated within the matrix and evaluate the safety of their use on *in vivo* models.

Fluorescence Intensity Assays

Fluorescence intensity (FI) assays were performed to observe the effects of the free *C. m. molossus* venom and the Cs-Venom NPs, in the T-47D breast carcinoma cells. The venom of the *C. m. molossus* and Cs-Venom NPs (Fig. 8) lowered the FI of rhodamine 123, generally associated with cell death due to a compromised cell membrane (Darzynkiewicz *et al.*, 1982). Additionally, there were significant differences be-

Figure 7. MTT assays were performed with Cs-Blank and Cs-Venom NPs.
C. m. molossus venom and Cs-Venom NPs were both able to lower the cell viability of the T-47D breast carcinoma cells by >60% at 31.25 µg/mL. *Are shown for statistical differences ($p<0.005$).

Figure 8. Fluorescence intensity assays were performed with the black-tailed rattlesnake (*C. m. molossus*) venom, Cs-Venom NPs, and Cs-Blank NPs stained with Rhodamine.
A decrease in fluorescence intensity indicates the death of cells. *Are shown for statistical differences ($p<0.005$). No significant differences were observed between the snake venom and Cs-Venom NPs.

tween the FI of the Cs-Blank NPs and snake venom and Cs-Venom NPs.

Several studies have shown how some snake venom toxins have specific interactions at cell membranes. Suhr and Kim (Suhr & Kim, 1996) reported how some LAAOs presented specificity, and thus, they observed different cytotoxic levels for different cell lines. It can be observed in Fig. 8, that the venom significantly affects cell morphology, and as reported elsewhere, this could be due to the specific action of certain toxins like SVMPs, LAAOs, and PLA$_2$s, like the ones in Table 1. Park and others (Park *et al.*, 2009) reported the morphology changes and apoptosis induction in SK-N-MC and SK-N-SH, neuroblastoma cells, after *Vipera lebetina* snake venom internalization. These changes were probably caused by reactive oxygen species (ROS), due to rupture in the cell's membrane potential (Park *et al.*, 2009) or pore formation due to PLA$_2$s (Chwetzoff *et al.*, 1989; Cummings, 2007; Gutiérrez & Lomonte, 1995). Our results show clear and noticeable morphological changes consistent with the MTT cytotoxicity assays, where cell viability of ~30% was observed at a venom concentration of 31.25 μg/mL (Figs 3 and 7).

In contrast with the Cs-Blank NPs (Fig. 8), no distinctive morphology changes were observed. The data obtained through the MTT assay of said NPs (Fig. 7) shows no apparent cytotoxic effect of the blank NPs. The FI assay shows that the Cs-Venom NPs could deliver the venom of *C. m. molossus* inside them. This study has contributed to the development of new potential anti-cancer drugs. The use of snake venom against tumor cells could be a viable option to treat this type of disease, as supported by the presented data.

CONCLUSIONS

It was demonstrated that the northern black-tailed rattlesnake (*C. m. molossus*) venom (formed majorly by VAP2A, Ruberlysin, Apoxin I, and Phospholipase A2_2) maintains cytotoxic activity against the T-47D breast carcinoma cell line after a chitosan NPs synthesis process. Cs-Venom (EE% of 48.29%) NPs presented a smooth and semi-spherical morphology with an average size of ~415 nm and ζ-potential of +28 mV. Cs-Venom NPs did not have hemolytic activity in human RBC (HA < 10%), especially at lower concentrations [0.187 mg/mL]. FI assays showed that the snake venom and Cs-Venom NPs both induced changes in cell morphology by compromising the cell mitochondria membrane potential. Although more research and data are required, for our results, the black-tailed rattlesnake (*C. m. molossus*) venom-loaded in the chitosan polymeric NPs appears to be a promising candidate to be researched for cancer pharmaceuticals.

Conflicts of interest

Authors declare no conflicts of interest.

REFERENCES

Aftab S, Shah A, Nadhman A, Kurbanoglu S, Aysıl Ozkan S, Dionysiou DD, Shukla SS, Aminabhavi TM (2018) Nanomedicine: An effective tool in cancer therapy. *Int J Pharmaceutics* **540**: 132–149. https://doi.org/10.1016/j.ijpharm.2018.02.007

Agarwal S, Mohamed MS, Mizuki T, Maekawa T, Kumar DS (2019) Chlorotoxin modified morusin–PLGA nanoparticles for targeted glioblastoma therapy. *J Mater Chem B* **7**: 5896–5919. https://doi.org/10.1039/C9TB01131E

Ahmed TA, Aljaeid BM (2016) Preparation, characterization, and potential application of chitosan, chitosan derivatives, and chitosan metal nanoparticles in pharmaceutical drug delivery. *Drug Des Devel Ther* **10**: 483–507. https://doi.org/10.2147/DDDT.S99651

Alaseem A, Alhazzani K, Dondapati P, Alobid S, Bishayee A, Rathinavelu A (2019) Matrix Metalloproteinases: A challenging paradigm of cancer management. *Seminars Cancer Biol* **56**: 100–115. https://doi.org/10.1016/j.semcancer.2017.11.008

Al-Sadoon MK, Rabah DM, Badr G (2013) Enhanced anticancer efficacy of snake venom combined with silica nanoparticles in a murine model of multiple human myelomas: Molecular targets for cell cycle arrest and apoptosis induction. *Cell Immunol* **284**: 129–138. https://doi.org/10.1016/j.cellimm.2013.07.016

Amin K, Dannenfelser R-M (2006) In vitro hemolysis: Guidance for the pharmaceutical scientist. *J Pharm Sci* **95**: 1173–1176. https://doi.org/10.1002/jps.20627

Argüelles-Monal WM, Lizardi-Mendoza J, Fernández-Quiroz D, Recillas-Mota MT, Montiel-Herrera M (2018) Chitosan derivatives: introducing new functionalities with a controlled molecular architecture for innovative materials. *Polymers* **10**: 342. https://doi.org/10.3390/polym10030342

Arvelo F, Cotte C (2006) Metalloproteinases in tumor progression. Review. *Invest Clin* **47**: 185–205

Azevedo FVPV, Lopes DS, Cirilo Gimenes SN, Achê DC, Vecchi L, Alves PT, Guimarães D de O, Rodrigues RS, Goulart LR, Rodrigues V de M, Yoneyama KAG (2016) Human breast cancer cell death induced by BnSP-6, a Lys-49 PLA2 homologue from Bothrops pauloensis venom. *Int J Biol Macromol* **82**: 671–677. https://doi.org/10.1016/j.ijbiomac.2015.10.080

Badr G, Al-Sadoon MK, Rabah DM (2013) Therapeutic efficacy and molecular mechanisms of snake (*Walterinnesia aegyptia*) venom-loaded silica nanoparticles in the treatment of breast cancer- and prostate cancer-bearing experimental mouse models. *Free Radic Biol Med* **65**: 175–189. https://doi.org/10.1016/j.freeradbiomed.2013.06.018

Bénard-Valle M, Carbajal-Saucedo A, de Roodt A, López-Vera E, Alagón A (2014) Biochemical characterization of the venom of the coral snake *Micrurus tener* and comparative biological activities in the mouse and a reptile model. *Toxicon* **77**: 6–15. https://doi.org/10.1016/j.toxicon.2013.10.005

Biswas A, Gomes A, Sengupta J, Datta P, Singha S, Dasgupta AK, Gomes A (2012) Nanoparticle-conjugated animal venom-toxins and their possible therapeutic potential. *J Venom Res* **3**: 15–21

Biswas AK, Islam MR, Choudhury ZS, Mostafa A, Kadir MF (2014) Nanotechnology-based approaches in cancer therapeutics. *Adv Nat Sci Nanosci Nanotechnol* **5**: 043001. https://doi.org/10.1088/2043-6262/5/4/043001

Boldrini-França J, Pinheiro-Junior EL, Peigneur S, Pucca MB, Cerni FA, Borges RJ, Costa TR, Carone SEI, Fontes MR de M, Sampaio SV, Arantes EC, Tytgat J (2020) Beyond hemostasis: a snake venom serine protease with potassium channel blocking and potential antitumor activities. *Sci Rep* **10**: 4476. https://doi.org/10.1038/s41598-020-61258-x

Borja M, Neri-Castro E, Pérez-Morales R, Strickland J, Ponce-López R, Parkinson C, Espinosa-Fematt J, Sáenz-Mata J, Flores-Martínez E, Alagón A, Castañeda-Gaytán G (2018a) Ontogenetic change in the venom of mexican black-tailed rattlesnakes (*Crotalus molossus nigrescens*). *Toxins* **10**: 501. https://doi.org/10.3390/toxins10120501

Borja M, Neri-Castro E, Castañeda-Gaytán G, Strickland JL, Parkinson CL, Castañeda-Gaytán J, Ponce-López R, Lomonte B, Olvera-Rodríguez A, Alagón A, Pérez-Morales R (2018b) Biological and proteolytic variation in the venom of *Crotalus scutulatus* scutulatus from Mexico. *Toxins* **10**: 35. https://doi.org/10.3390/toxins10010035

Bradford MM (1976) A rapid and sensitive method for the quantitation of microgram quantities of protein utilizing the principle of protein-dye binding. *Anal Biochem* **72**: 248–254. https://doi.org/10.1006/abio.1976.9999. PMID: 942051

Calderon LA, Sobrinho JC, Zaqueo KD, de Moura AA, Grabner AN, Mazzi MV, Marcussi S, Nomizo A, Fernandes CFC, Zuliani JP, Carvalho BMA, da Silva SL, Stábeli RG, Soares AM (2014) Antitumoral activity of snake venom proteins: new trends in cancer therapy. *BioMed Res Int* **2014**: 1–19. https://doi.org/10.1155/2014/203639

Calvete JJ, Fasoli E, Sanz L, Boschetti E, Righetti PG (2009) Exploring the venom proteome of the western diamondback rattlesnake, *Crotalus atrox*, via snake venomics and combinatorial peptide ligand library approaches. *J. Proteome Res* **8**: 3055–3067. https://doi.org/10.1021/pr900249q

Calvo P, Remuñán-López C, Vila-Jato JL, Alonso MJ (1997) Novel hydrophilic chitosan-polyethylene oxide nanoparticles as protein carriers. *J Appl Polymer Sci* **63**: 125–132. https://doi.org/10.1002/(SICI)1097-4628(19970103)63:1<125::AID-APP13>3.0.CO;2-4

Carreño-Gómez B, Duncan R (1997) Evaluation of the biological properties of soluble chitosan and chitosan microspheres. *Int J Pharm* **148**: 231–240. https://doi.org/10.1016/S0378-5173(96)04847-8

Castro EN, Lomonte B, del Carmen Gutiérrez M, Alagón A, Gutiérrez JM (2013) Intraspecies variation in the venom of the rattlesnake *Crotalus simus* from Mexico: Different expression of crotoxin results in highly variable toxicity in the venoms of three subspecies. *J Proteomics* **87**: 103–121. https://doi.org/10.1016/j.jprot.2013.05.024

Chellapandi P (2014) Structural, functional and therapeutic aspects of snake venom metalloproteinases. *MROC* **11**: 28–44. https://doi.org/10.2174/1570193X1101140402100707

Chwetzoff S, Tsunasawa S, Sakiyama F, Ménez A (1989) Nigexine, a phospholipase A2 from cobra venom with cytotoxic properties not related to esterase activity. Purification, amino acid sequence, and biological properties. *J Biol Chem* **264**: 13289–13297

Coates J (2000) Interpretation of Infrared Spectra, A Practical Approach. In *Infrared Spectroscopy*. https://doi.org/10.1002/9780470027318.a5606

Corin RE, Viskatis LJ, Vidal JC, Etcheverry MA (1993) Cytotoxicity of crotoxin on murine erythroleukemia cells *in vitro*. *Invest New Drugs* **11**: 11–15. https://doi.org/10.1007/BF00873905

Cummings BS (2007) Phospholipase A2 as targets for anti-cancer drugs. *Biochem Pharmacol* **74**: 949–959. https://doi.org/10.1016/j.bcp.2007.04.021

Danhier F, Ansorena E, Silva JM, Coco R, Le Breton A, Préat V (2012) PLGA-based nanoparticles: An overview of biomedical applications. *J Controlled Release* **161**: 505–522. https://doi.org/10.1016/j.jconrel.2012.01.043

Darzynkiewicz Z, Traganos F, Staiano-Coico L, Kapuscinski J, Melamed MR (1982) Interactions of rhodamine 123 with living cells studied by flow cytometry. *Cancer Res* **42**: 799–806

Diaz-Galvez KR, Teran-Saavedra NG, Burgara-Estrella AJ, Fernandez-Quiroz D, Silva-Campa E, Acosta-Elias M, Sarabia-Sainz HM, Pedroza-Montero MR, Sarabia-Sainz JA (2019) Specific capture of glycosylated graphene oxide by an asialoglycoprotein receptor: a strategic approach for liver-targeting. *RSC Adv* **9**: 9899–9906. https://doi.org/10.1039/C8RA09732A

DiPietrantonio AM, Hsieh T, Wu JM (1999) Activation of caspase 3 in HL-60 cells exposed to hydrogen peroxide. *Biochem Biophys Res Commun* **255**: 477–482. https://doi.org/10.1006/bbrc.1999.0208

Du X-Y, Clemetson KJ (2002) Snake venom L-amino acid oxidases. *Toxicon* **40**: 659–665. https://doi.org/10.1016/s0041-0101(02)00102-2. Erratum in: *Toxicon* 2002 **40**: 1381. PMID: 12175601

Ebrahimian V (2013) Characterization of red diamondback rattlesnake venom proteins on cell death and function. *Browse all Theses and Dissertations* 1166. https://corescholar.libraries.wright.edu/etd_all/1166

Fernández-Quiroz D, Loya-Duarte J, Silva-Campa E, Argüelles-Monal W, Sarabia-Sainz A-í, Lucero-Acuña A, del Castillo-Castro T, San Román J, Lizardi-Mendoza J, Burgara-Estrella AJ, Castaneda B, Soto-Puebla D, Pedroza-Montero M (2019) Temperature stimuli-responsive nanoparticles from chitosan-graft-poly(N-vinylcaprolactam) as a drug delivery system. *J Appl Polymer Sci* **136**: 47831. https://doi.org/10.1002/app.47831

Furtado MFD, Travaglia-Cardoso SR, Rocha MMT (2006) Sexual dimorphism in venom of *Bothrops jararaca* (Serpentes: Viperidae). *Toxicon* **48**: 401–410. https://doi.org/10.1016/j.toxicon.2006.06.005

Gallegos-Tabanico A, Sarabia-Sainz JA, Sarabia-Sainz HM, Carrillo Torres R, Guzman-Partida AM, Monfort GR-C, Silva-Campa E, Burgara-Estrella AJ, Angulo-Molina A, Acosta-Elias M, Pedroza-Montero M, Vazquez-Moreno L (2017) Molecular recognition of glyconanoparticles by RCA and *E. coli* K88 – designing transports for targeted therapy. *Acta Biochim Pol* **64**: 671–677. https://doi.org/10.18388/abp.2017_1639

Gláucia-Silva F, Torres-Rêgo M, Rocha Soares KS, Damasceno IZ, Tambourgi DV, Silva-Júnior AA da, Fernandes-Pedrosa M de F (2018) A biotechnological approach to immunotherapy: Antivenom against Crotalus durissus cascavella snake venom produced from biodegradable nanoparticles. *Int J Biol Macromol* **120**: 1917–1924. https://doi.org/10.1016/j.ijbiomac.2018.09.203

Goycoolea FM, Lollo G, Remuñán-López C, Quaglia F, Alonso MJ (2009) Chitosan-alginate blended nanoparticles as carriers for the transmucosal delivery of macromolecules. *Biomacromolecules* **10**: 1736–1743. https://doi.org/10.1021/bm9001377

Gutiérrez J, Lomonte B (1995) Phospholipase A2 myotoxins from Bothrops snake venoms. *Toxicon* **33**: 1405–1424. https://doi.org/10.1016/0041-0101(95)00085-Z

Gutiérrez JM, Rucavado A (2000) Snake venom metalloproteinases: Their role in the pathogenesis of local tissue damage. *Biochimie* **82**: 841–850. https://doi.org/10.1016/S0300-9084(00)01163-9

Zou Alfagharian H, Mohammadpour Dounighi N (2009) Encapsulation of Naja – Naja oxiana snake venom into poly (lactide-co-glycolide) microspheres. *Arch Razi Institute* **64**: 101–107

Hare JI, Lammers T, Ashford MB, Puri S, Storm G, Barry ST (2017) Challenges and strategies in anti-cancer nanomedicine development: An industry perspective. *Adv Drug Delivery Rev* **108**: 25–38. https://doi.org/10.1016/j.addr.2016.04.025

Hayashi MAF, Oliveira EB, Kerkis I, Karpel RL (2012) Crotamine: A novel cell-penetrating polypeptide nanocarrier with potential anti-cancer and biotechnological applications. In *Nanoparticles in Biology and Medicine*. Soloviev M ed, pp 337–352. Totowa, NJ: Humana Press. https://doi.org/10.1007/978-1-61779-953-2_28

Huerta-Ocampo JA, Barrera-Pacheco A, Mendoza-Hernández CS, Espitia-Rangel E, Mock H-P, Barba de la Rosa AP (2014) Salt stress-induced alterations in the root proteome of *Amaranthus cruentus* L. *J Proteome Res* **13**: 3607–3627. https://doi.org/10.1021/pr500153m

Kamiguti AS, Zuzel M, Theakston RDG (1998) Snake venom metalloproteinases and disintegrins: Interactions with cells. *Braz J Med Biol Res* **31**: 853–862. https://doi.org/10.1590/S0100-879X1998000700001

Karpel RL, da Silva Liberato M, Campeiro JD, Bergeon L, Szychowski B, Butler A, Marino G, Cusic JF, de Oliveira LCG, Oliveira EB, de Farias MA, Portugal RV, Alves WA, Daniel M-C, Hayashi MAF (2018) Design and characterization of crotamine-functionalized gold nanoparticles. *Colloids and Surfaces B: Biointerfaces* **163**: 1–8. https://doi.org/10.1016/j.colsurfb.2017.12.013

Kerkis I, Hayashi MAF, Prieto da Silva ARB, Pereira A, De Sá Júnior PL, Zaharenko AJ, Rádis-Baptista G, Kerkis A, Yamane T (2014) State of the art in the studies on crotamine, a cell-penetrating peptide from South American rattlesnake. *BioMed Res Int* **2014**: 1–9. https://doi.org/10.1155/2014/675985

Laemmli UK (1970) Cleavage of structural proteins during the assembly of the head of bacteriophage T4. *Nature* **227**: 680–685. https://doi.org/10.1038/227680a0

Lee KJ, Kim YK, Krupa M, Nguyen AN, Do BH, Chung B, Vu TTT, Kim SC, Choe H (2016) Crotamine stimulates phagocytic activity by inducing nitric oxide and TNF-α *via* p38 and NFκ-B signaling in RAW 264.7 macrophages. *BMB Reports* **49**: 185–190. https://doi.org/10.5483/BMBRep.2016.49.3.271

Li J, Cai C, Li J, Li J, Li J, Sun T, Wang L, Wu H, Yu G (2018a) Chitosan-based nanomaterials for drug delivery. *Molecules* **23**: https://doi.org/10.3390/molecules23102661

Li L, Huang J, Lin Y (2018b) Snake venoms in cancer therapy: Past, present and future. *Toxins* **10**: 346. https://doi.org/10.3390/toxins10090346

Luque-Alcaraz AG, Lizardi-Mendoza J, Goycoolea FM, Higuera-Ciapara I, Argüelles-Monal W (2016) Preparation of chitosan nanoparticles by nanoprecipitation and their ability as a drug nanocarrier. *RSC Adv* **6**: 59250–59256. https://doi.org/10.1039/C6RA06563E

Macias-Rodríguez EF, Martínez-Martínez A, Gatica-Colima A, Bojórquez-Rangel G, Plenge-Tellechea LF (2014) Análisis comparativo de la actividad hemolítica entre las subespecies *Crotalus molossus y Crotalus molossus nigrescens*. *Revista Bio Ciencias* **2**: 302–312. https://doi.org/10.15741/revbio.02.04.08

Maeda H (2021) The 35th Anniversary of the discovery of EPR effect: A new wave of nanomedicines for tumor-targeted drug delivery-personal remarks and future prospects. *J Pers Med* **11**: 229. https://doi.org/10.3390/jpm11030229

Marinovic MP, Mas CD, Monte GG, Felix D, Campeiro JD, Hayashi MAF (2017) Crotamine: function diversity and potential applications. In *Snake Venoms*. Inagaki H, Vogel C-W, Mukherjee AK, Rahmy TR eds, pp 265–293. Dordrecht: Springer Netherlands. https://doi.org/10.1007/978-94-007-6410-1_28

Masuda S, Hayashi H, Araki S (1998) Two vascular apoptosis-inducing proteins from snake venom are members of the metalloprotease/disintegrin family. *Eur J Biochem* **253**: 36–41. https://doi.org/10.1046/j.1432-1327.1998.2530036.x

Meléndez-Martínez D, Macías-Rodríguez E, Vázquez-Briones R, López-Vera E, Cruz-Pérez MS, Vargas-Caraveo A, Gatica-Colima A, Plenge-Tellechea LF (2017) *In vitro* hemotoxic, α-neurotoxic and vasculotoxic effects of the Mexican black-tailed rattlesnake (*Crotalus molossus nigrescens*) venom. *J Venom Res* **8**: 2854003

Mir M, Ahmed N, Rehman A ur (2017) Recent applications of PLGA based nanostructures in drug delivery. *Colloids Surfaces B: Biointerfaces* **159**: 217–231. https://doi.org/10.1016/j.colsurfb.2017.07.038

Modahl CM, Mackessy SP (2016) Full-length venom protein cDNA sequences from venom-derived mRNA: exploring compositional variation and adaptive multigene evolution. *PLoS Negl Trop Dis* **10**: e0004587. https://doi.org/10.1371/journal.pntd.0004587

Mohammadpourdounighi N, Behfar A, Ezabadi A, Zolfagharian H, Heydari M (2010) Preparation of chitosan nanoparticles containing Naja naja oxiana snake venom. *Nanomedicine: Nanotechnol Biol Med* **6**: 137–143. https://doi.org/10.1016/j.nano.2009.06.002

Morales-Amparano MB, Ramos-Clamont Montfort G, Baqueiro-Peña I, Robles-Burgueño M del R, Vázquez-Moreno L, Huerta-Ocampo JÁ (2019) Proteomic response of *Saccharomyces boulardii* to simulated gastrointestinal conditions and encapsulation. *Food Sci Biotechnol* **28**: 831–840. https://doi.org/10.1007/s10068-018-0508-9

Naser M, Rezvan Y, Hossein Z (2015) A new antigen delivery vehicle candidate: Orthochirus iranus scorpion venom entrapped in chitosan nanoparticles. *BJPR* **7**: 264–275. https://doi.org/10.9734/BJPR/2015/16667

Omar Zaki SS, Ibrahim MN, Katas H (2015) Particle size affects concentration-dependent cytotoxicity of chitosan nanoparticles towards mouse hematopoietic stem cells. *J Nanotechnol* **2015**: 1–5. https://doi.org/10.1155/2015/919658

Park MH, Son DJ, Kwak DH, Song HS, Oh K-W, Yoo H-S, Lee YM, Song MJ, Hong JT (2009) Snake venom toxin inhibits cell growth through induction of apoptosis in neuroblastoma cells. *Arch Pharm Res* **32**: 1545–1554. https://doi.org/10.1007/s12272-009-2106-0

Pedroso-Santana S, Fleitas-Salazar N (2020) Ionotropic gelation method in the synthesis of nanoparticles/microparticles for biomedical purposes. *Polymer Int* **69**: 443–447. https://doi.org/10.1002/pi.5970

Peniche C, Argüelles-Monal W, Goycoolea FM (2008) Chapter 25 – Chitin and chitosan: major sources, properties and applications. In *Monomers, Polymers and Composites from Renewable Resources*. Belgacem MN, Gandini A eds, pp 517–542. Amsterdam: Elsevier. https://doi.org/10.1016/B978-0-08-045316-3.00025-9

Quiñones JP, Peniche H, Peniche C (2018) Chitosan based self-assembled nanoparticles in drug delivery. *Polymers* **10**: 235. https://doi.org/10.3390/polym10030235

Rampino A, Borgogna M, Blasi P, Bellich B, Cesàro A (2013) Chitosan nanoparticles: Preparation, size evolution and stability. *Int J Pharm* **455**: 219–228. https://doi.org/10.1016/j.ijpharm.2013.07.034

Riegger BR, Bäurer B, Mirzayeva A, Tovar GEM, Bach M (2018) A systematic approach of chitosan nanoparticle preparation via emulsion crosslinking as potential adsorbent in wastewater treatment. *Carbohydrate Polymers* **180**: 46–54. https://doi.org/10.1016/j.carbpol.2017.10.002

Rivas-Mercado EA, Garza-Ocañas L (2017) Disintegrins obtained from snake venom and their pharmacological potential. *Medicina Universitaria* **19**: 32–37. https://doi.org/10.1016/j.rmu.2017.02.004

Rizvi SAA, Saleh AM (2018) Applications of nanoparticle systems in drug delivery technology. *Saudi Pharm Jl* **26**: 64–70. https://doi.org/10.1016/j.jsps.2017.10.012

Samel M, Vija H, Rönnholm G, Siigur J, Kalkkinen N, Siigur E (2006) Isolation and characterization of an apoptotic and platelet aggregation inhibiting L-amino acid oxidase from *Vipera berus berus* (common viper) venom. *Biochim Biophys Acta (BBA) – Proteins and Proteomics* **1764**: 707–714. https://doi.org/10.1016/j.bbapap.2006.01.021

Sarmento B, Ferreira D, Veiga F, Ribeiro A (2006) Characterization of insulin-loaded alginate nanoparticles produced by ionotropic pre-gelation through DSC and FTIR studies. *Carbohydrate Polymers* **66**: 1–7. https://doi.org/10.1016/j.carbpol.2006.02.008

Sawtarie N, Cai Y, Lapitsky Y (2017) Preparation of chitosan/tripolyphosphate nanoparticles with highly tunable size and low polydispersity. *Colloids and Surfaces B: Biointerfaces* **157**: 110–117. https://doi.org/10.1016/j.colsurfb.2017.05.055

Soares K, Gláucia-Silva F, Daniele-Silva A, Torres-Rêgo M, Araújo N, Menezes Y, Damasceno I, Tambourgi D, da Silva-Júnior A, Fernandes-Pedrosa M (2018) Antivenom production against *Bothrops jararaca* and *Bothrops erythromelas* snake venoms using cross-linked chitosan nanoparticles as an immunoadjuvant. *Toxins* **10**: 158. https://doi.org/10.3390/toxins10040158

Subhan MA, Yalamarty SSK, Filipczak N, Parveen F, Torchilin VP (2021) Recent advances in tumor targeting *via* EPR effect for cancer treatment. *J Pers Med* **11**: 571. https://doi.org/10.3390/jpm11060571

Suhr S-M, Kim D-S (1996) Identification of the snake venom substance that induces apoptosis. *Biochem Biophys Res Communi* **224**: 134–139. https://doi.org/10.1006/bbrc.1996.0996

Takeya H, Onikura A, Nikai T, Sugihara H, Iwanaga S (1990) Primary structure of a hemorrhagic metalloproteinase, HT-2, isolated from the venom of *Crotalus ruber ruber*. *J Biochem* **108**: 711–719. https://doi.org/10.1093/oxfordjournals.jbchem.a123270

Tang C-H, Yang R-S, Liu C-Z, Huang T-F, Fu W-M (2004) Differential susceptibility of osteosarcoma cells and primary osteoblasts to cell detachment caused by snake venom metalloproteinase protein. *Toxicon* **43**: 11–20. https://doi.org/10.1016/j.toxicon.2003.10.008

Tasoulis T, Isbister G (2017) A review and database of snake venom proteomes. *Toxins* **9**: 290. https://doi.org/10.3390/toxins9090290

Teran-Saavedra N, Sarabia-Sainz J, Silva-Campa E, Burgara-Estrella A, Guzmán-Partida A, Ramos-Clamont Montfort G, Pedroza-Montero M, Vazquez-Moreno L (2019) Lactosylated albumin nanoparticles: potential drug nanovehicles with selective targeting toward an *in vitro* model of hepatocellular carcinoma. *Molecules* **24**: 1382. https://doi.org/10.3390/molecules24071382

Torii S, Naito M, Tsuruo T (1997) Apoxin I, a novel apoptosis-inducing factor with L-amino acid oxidase activity purified from western diamondback rattlesnake venom. *J Biol Chem* **272**: 9539–9542. https://doi.org/10.1074/jbc.272.14.9539

Torii S, Yamane K, Mashima T, Haga N, Yamamoto K, Fox JW, Naito M, Tsuruo T (2000) Molecular cloning and functional analysis of apoxin I, a snake venom-derived apoptosis-inducing factor with L-amino acid oxidase activity. *Biochemistry* **39**: 3197–3205. https://doi.org/10.1021/bi992416z

Tran S, DeGiovanni P-J, Piel B, Rai P (2017) Cancer nanomedicine: a review of recent success in drug delivery. *Clin Trans Med* **6**: 44. https://doi.org/10.1186/s40169-017-0175-0

Wu J, Wang Y, Yang H, Liu X, Lu Z (2017) Preparation and biological activity studies of resveratrol loaded ionically cross-linked chitosan-TPP nanoparticles. *Carbohydrate Polymers* **175**: 170–177. https://doi.org/10.1016/j.carbpol.2017.07.058

Zhang Y-J, Wang J-H, Lee W-H, Wang Q, Liu H, Zheng Y-T, Zhang Y (2003) Molecular characterization of *Trimeresurus stejnegeri* venom L-amino acid oxidase with potential anti-HIV activity. *Biochem Biophys Res Commun* **309**: 598–604. https://doi.org/10.1016/j.bbrc.2003.08.044

Zhou Y, Li J, Lu F, Deng J, Zhang J, Fang P, Peng X, Zhou S-F (2015) A study on the hemocompatibility of dendronized chitosan derivatives in red blood cells. *Drug Des Devel Ther* **9**: 2635–2645. https://doi.org/10.2147/DDDT.S77105